Identification of hydrocarbon contamination in low porosity marble samples using ac conductivity time-series

G. HLOUPIS [(1,2)], **I. STAVRAKAS**[(3)], **D. TRIANTIS** [(3)], **F. VALLIANATOS** [(1)], **J. STONHAM** [(2)]

(1) Technological Educational Institute of Crete
Romanou 3 – 73133 – Chania – GREECE

(2) Department of Electronic and Computer Engineering
Brunel University - Uxbridge – Middlesex – UB8 3PH – UNITED KINGDOM

(3) Department of Electronics,
Technological Educational Institute of Athens
Ag Spyridonos – 12210 - Athens – GREECE

Abstract: In this work an attempt is made to compare the spectrum of ac conductivity time series, on various frequencies, of low porosity geomaterial samples that were contaminated by hydrocarbon compounds and others that were not influenced by contaminators. The used geomaterials were Mt. Penteli marbles. The power spectral density was calculated for both, contaminated and not, samples with the aid of wavelet transform in order to achieve time-frequency localization. The shape of the log-log plot of the power spectral density show clear differences between the contaminated samples and those that had not been affected by the hydrocarbon contamination compounds.

1 Introduction

Measurements of the dielectric properties, on geomaterials, by the use of broadband dielectric spectroscopy can provide information about pre-applied physical processes and chemical characteristics of geomaterials [1,2]. Specifically, dielectric measurements have been performed to study water content of soils [3-5] hydrocarbon contamination [1,6], previously applied physical processes such as hydration [7] and pressure [8]. The main advantage of this technique is that it is a non-destructive testing method, enabling sample re-examination.

In previous studies [9,10] metastable phenomena yielded to dynamical processes like temperature change have been studied using dielectric spectroscopy and specifically ac conductivity time series analysis. During these works power spectral densities have been calculated by the use of Fourier transform.

Others have studied and proved that hydrocarbon contamination and water content, have different fingerprints on dielectric data of ground rocks [6].

In the present work an innovative attempt took place to study hydrocarbon contamination by the use of ac conductivity time series on various frequencies applied on geomaterials like Mt. Penteli marbles. These marbles are characterized of extremely low porosity [11], with few connected pores, and liquid contamination factors limitedly penetrate rock mass. The above makes more interesting the study of the applicability of bulk ac conductivity measurements on such materials to investigate hydrocarbon compounds contamination. Thus, time series of ac conductivity were recorded and the data was analyzed using Wavelet Transform (WT). Since stationarity of the time series is not verified, it is safer to study the ac conductivity time series with the aid of wavelet transform [12] rather than Fourier Transform.

2 Theoretical background

2.1 Data analysis of ac conductivity time series.

Using Dielectric Spectroscopy technique the values of capacitance, C, and conductance, G, are directly provided by the measuring system (Agilent 4284A). Ac conductivity, σ_{ac}, is calculated when applying conductance, G, value to the following formula:

$$\sigma_{ac} = G\frac{d}{A} \tag{1}$$

where d stands for the thickness of the sample and A stands for the electrodes area when this is greater than the cross sectional area of the sample.

Using capacitance, C, the real part of relative permittivity, $\varepsilon_r^{'}$, is calculated by the use of the formula

$$\varepsilon_r^{'} = \frac{C}{\varepsilon_0(A/d)} \tag{2}$$

while ε_0 corresponds to the vacuum permittivity.

It is expected, since for each sample ac conductivity time series are measured for more than one frequency, to exhibit different absolute values of conductance. This is due to the universal power law that dominates conductivity behavior with respect to frequency:

$$\sigma_{ac}(f) = \sigma_{dc} + Bf^n \tag{3}$$

where σ_{dc} is the dc conductivity B is a parameter depending on temperature and pressure and exponent n takes values between 0 and 1

Typical time series can be created by sampling, with constant rate, single frequency ac conductivity. In order to be able to study the time series the data was corrected by removing constant trend calculating this way the fluctuations of ac conductivity by applying:

$$\Delta\sigma_{ac}(t) = \sigma_{ac}(t) - <\sigma_{ac}(t)> \tag{4}$$

An observed signal is strict-sense stationary if the joint distribution of any set of samples does not depend on the sample's placement. Consequently, first order cumulative distribution functions, e.g., mean and variance of the signal are constant. Furthermore, second order cumulative distribution functions (such as autocorrelation and autocovariance) depend only on the distance in placement. For example, a Gaussian process is strict-sense stationary since it is completely specified by its mean and covariance function. Stationarity was investigated for the time series produced from this process in order to evaluate the need for appropriate time-frequency analysis method. Stationarity investigation was done by examining one first order cumulative attribute (amplitude distribution) and one second order cumulative function (autocorrelation).

2.2 Wavelet transform (WT)

The Continuous Wavelet Transform (CWT) is used to decompose a signal into wavelets. Whereas the Fourier transform decomposes a signal into infinite length sines and cosines, effectively losing all time-localization information, the CWT's basis functions are scaled (by s) and shifted (by x) versions of the time-localized mother wavelet. The CWT is a convolution of the data sequence with a scaled and translated version of the mother wavelet, the ψ function [13].

In the CWT, for each value of the scale used, the correlation between the scaled wavelet and successive segments of the data stream is computed. The convolutions can be done up to N times at each scale, and must be done all N times if the FFT is used. The CWT consists of N spectral values for each scale used, each of these requiring an inverse FFT.

The selection of the mother wavelet function is critical for the results that are expected to be derived. In this analysis derivative of Gaussian (DOG) wavelet, which uses real and optimally localised in both space and frequency, was chosen. The DOG wavelet is defined as:

$$\psi_0(x) = \frac{d^m}{dx^m}\left(e^{\frac{-x^2}{2}}\right) \tag{5}$$

where the order m of the wavelet is defined as the order of differentiation. The peak frequency (ω_c) of DOG wavelets at scale $s=0$ is given [14] by:

$$\omega_c = \sqrt{m} \tag{6}$$

Estimates of the power spectrum of a signal using wavelet coefficients can be generated. The wavelet approach in deriving a spectrum is similar to Fourier approach but time/scale decomposition is used instead of time/frequency. In contrast to the Fourier power spectrum, the wavelet power spectrum provides information with the local spectral content of the signal. The local wavelet power spectrum P is defined as:

$$P(x,s) = \frac{1}{N}|W(x,s)|^2 \tag{7}$$

The values $P(x,s)$ are an estimate of the signal power in a region of influence defined by spatial width Δc at about b and by frequency bandwidth Δc around mean frequency ω_c/s at scale s. To improve the accuracy of the estimates the local wavelet

power spectrum is averaged over a range of 2K+1 adjoining values to produce the averaged wavelet power spectrum (AWS) [14]:

$$P_{av}(x_n, s) = \frac{1}{R} \sum_{j=n-\frac{K}{2}}^{n+\frac{K}{2}} P(x_j, s) \qquad (8)$$

In the limiting case, the summation is over the entire signal and we obtain the global wavelet power spectrum. This can be an estimate of the value of the periodogram at the mean frequency smoothed by the wavelet at scale *s*.

In practice the scale, *s,* and translation, *x*, can be associated with a corresponding frequency *ω*, and time, *t,* in order to be considered as a representation of the time-varying, localized energy spectrum for the given time series. The graphical representation of the above produces a 3D energy map showing the distribution of energy corresponding to each *x,s.* AWS can be obtained by integrating the energy map in time at each duration.

3 Experimental setup

The material used for the experiments was marble collected from Mt. Penteli. It is mainly composed of calcite (98%) and other minerals depending on the variety of the marble, such as muscovite, sericite and chlorite. Its density is 2.7 gr/cm^3. A basic characteristic of Penteli marble is its low porosity, approximately 0.4%. This fact makes more interesting the study of hydrocarbon contamination by the method of ac conductivity time series analysis. In this work the marble specimens were provided in the form of tablets of thickness t=6mm and cross-section A=400mm^2 approximately.

The experiments were conducted on two sets of samples. The first set contained samples without any previous contamination. The samples of the second set were artificially contaminated by hydrocarbon compounds. Contamination process was performed as follows: The samples of the one set were sunk in depth of 0.4m in controlled environment with clay. The clay was contaminated by liquid hydrocarbon compounds spray continuously for a period of two months. Two months after this process the samples were removed from the clay and their surface were cleaned in order to perform ac conductivity measurements.

Ac conductivity time series were conducted at 10KHz and 100KHz using the Agilent 4284A LCR meter, accompanied by Agilent 16451B test fixture and further supported by a computer for data recording, storage and analysis. The dielectric test fixture that was used to hold the specimen was protected by a cabin providing constant temperature (298K), inert atmosphere by continuous effusion of inert gas and also low humidity. The detailed experimental set-up is described in previous works [12]

The ac conductivity measurements were made with sensitivity of $\pm 10^{-9} S/m$. All the measurements were made at isothermal conditions ($298 \pm 0.3K$) controlled by PC. The sampling rate was 3samples/s giving a maximum detection frequency of 1.5Hz. For each sample and frequency a 3000 data points set was collected.

4 Results

The ac conductivity time series were corrected for line-trends. The produced time-series are illustrated below (fig.1, fig.2):
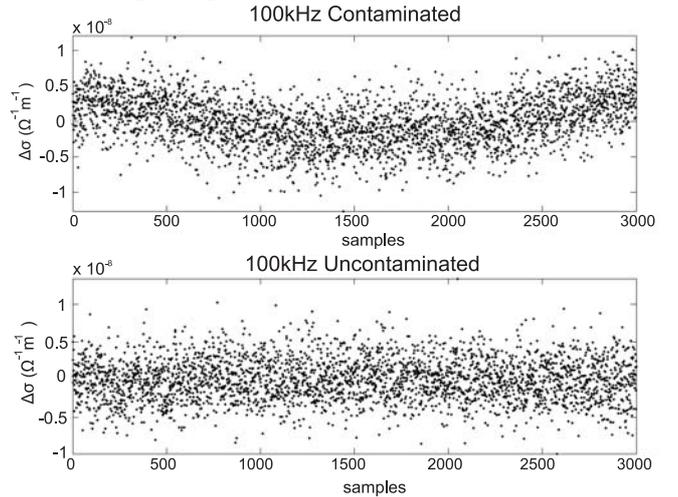
Fig. 1: Ac conductivity (100kHz) time series.
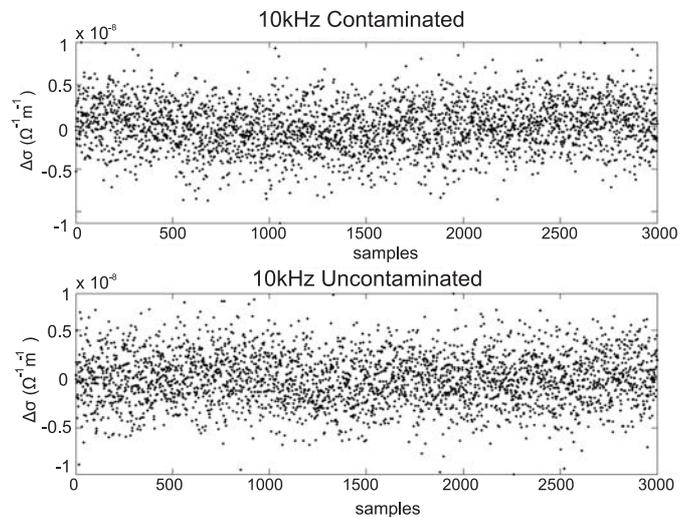
Fig. 2: Ac conductivity (10KHz) time series.

In order to quantify WT as an appropriate method for analysis, some simple tests are useful to investigate the existence of non-stationarity in our signals. The first one may be to observe the amplitude distribution. If the distribution is proved to be non-Gaussian then the signal is not strictly stationary [15-17]. Fig.3 illustrates the calculated histograms for each one of the time series. The second test is based on the shape of the autocorrelation function (ACF). If a time series is non-stationary then the ACF (after lag 1) will decrease slowly [17,18]. Fig.4 shows the produced ACFs.
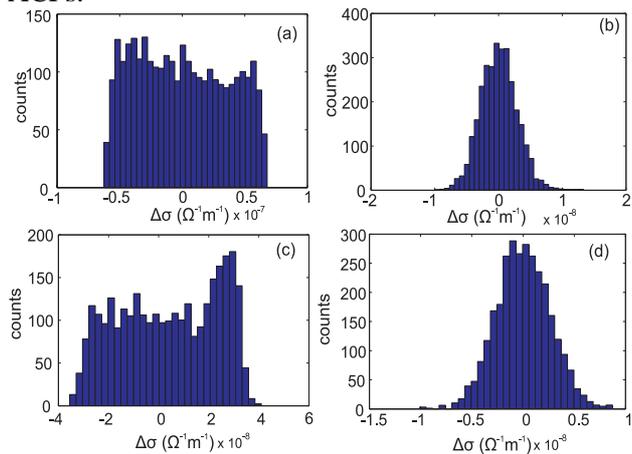
Fig. 3: Histograms of the detrended amplitude of the ac conductivity time series for a) 100kHz, contaminated sample, b) 100kHz, uncontaminated sample, c) 10kHz, contaminated sample, b) 10kHz, uncontaminated sample.
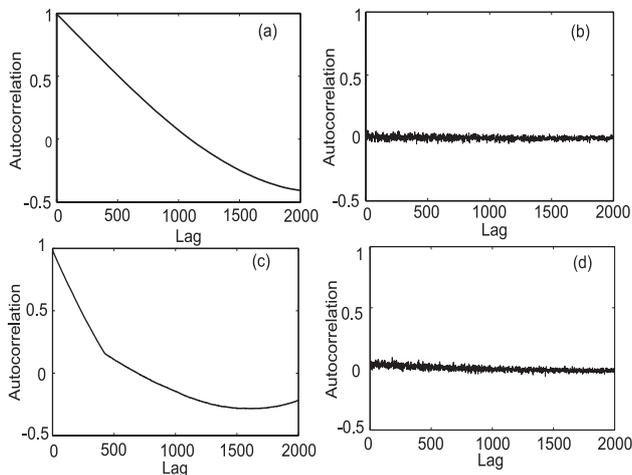
Fig. 4: ACFs for ac conductivity time series for a) 100kHz, contaminated sample, b) 100kHz, uncontaminated sample, c) 10kHz contaminated sample, b) 10kHz, uncontaminated sample.

Plot of Fig. 3 makes clear that ac conductivity distribution is not Gaussian. This fact manifests that the signal is not stationary. ACF tests were also applied to verify non-stationarity as this was concluded from distribution tests. Fig. 4 shows the

ACF of the contaminated samples to decrease slowly, which verifies that the signal is non-stationary. Since the two of the investigated time series proved to be non-stationary spectral analysis based on wavelet transform was chosen as more suitable than Fourier transform.

The wavelet spectrums calculated using WAVEPACK [14]. For each sample, contaminated and uncontaminated, the wavelet spectrum is calculated for both measured ac conductivity frequencies (10KHz and 100KHz). The produced spectrums in log-log plots of power spectral density vs. frequency are shown below (fig.5, fig.6)
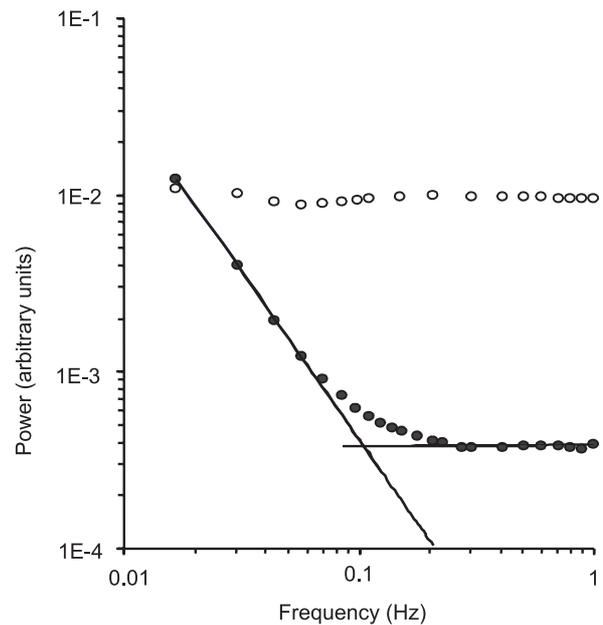
Fig. 5: AWS for uncontaminated (empty circle) and contaminated sample (solid circle) at 10KHz
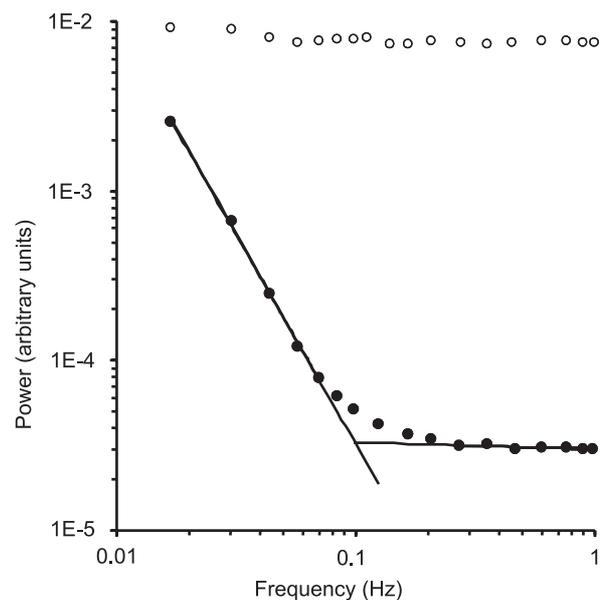
Fig. 6: AWS for uncontaminated (empty circle) and contaminated sample (solid circle) at 100KHz

From the above calculated wavelet spectrum a clear diversification between contaminated and uncontaminated samples in either measuring frequencies can be identified. The slope of the spectrum for the contaminated sample follows a rapid decrease as frequency increases and especially at the interval 0.01Hz to 0.15Hz. Contrary to that the slope of the spectrum for the uncontaminated sample shows a slow decrease which is by far different from the slope of contaminated sample. This behavior exists in 10KHz as well as at 100KHz.

Future work can acquire more ac conductivity measurements from different low porosity materials as well as from same samples with different level of contamination in order to identify the variation of spectrum's slope according to them.

5 Conclusion

The identification of hydrocardon contamination in low porosity materials with the aid of wavelet transform is presented. The calculation of power spectral densities in wavelet domain reveals an important diversification according to the slope spectrum between contaminated and uncontaminated samples. This promising result can guide us in a recognition scheme where we may identify polluted or contaminated materials using ac conductivity measurements and examining the slope of the wavelet spectrum from ac conductivity time series.

References:
[1] Kaya,A., Fang,H., *Identification of contaminated soils by dielectric constant and electrical conductivity*, Journal of Enviromental Engineering,1997, pp. 169-177
[2] Carrier,M., Soga,K., *A four terminal measurement system for measuring dielectric properties of clay at low frequencies*, Enginnering Geology 53, 1999, pp. 115-123
[3] S Capaccioli, M Lucchesi, R Casalini, P A Rolla and N Bona,*Influence of the wettability on the electrical response of microporous systems,* J. Phys. D: Appl. Phys. 33 (2000) 1036–1047.
[4] Kyritsis, A.; Siakantari, M.; Vassilikou-Dova, A.; Pissis, P.; Varotsos, P., *Dielectric and electrical properties of polycrystalline rocks at various hydration levels, Dielectrics and Electrical Insulation,* IEEE Transactions on [see also Electrical Insulation, IEEE Transactions on], Volume: 7 , Issue: 4 , Aug. 2000, pp.493 - 497
[5] Vassilikou-Dova, A.; Siakantari, M.; Kyritsis, A.; Varotsos, P.; Pissis, P., *The dependence of the dielectric behaviour of rocks on the water content Electrets,* 1999, ISE 10, Proceedings. 10th International Symposium, 22-24 Sept. 1999, pp.481 - 484
[6] Hallbauer-Zaborozhnaya, V., Kemenetsly, F., Shmidbauer, E., *Laboratory measurements of frequency dispersion of sedimentary rocks electric properties as applied to ground water hydrocarbon contamination,* 16th EM Induction Workshop, New Mexico, USA, June 16-22, 2002.
[7] Triantis, D., Stavrakas, I., Anastasiadis, C., Vallianatos, F., Kersaw, S*., Dielectric Spectroscopy in crustal rocks: Preliminary results from northeastern sicily (Italy) and the gulf of Corinth (Greece),* Bulletin of the Geological Society on Greece, vol. XXXVI, 2004, (in press)
[8] Triantis, D., Anastasiadis, C., Stavrakas, I., and Vallianatos, F., 2003. Dielectric characteristics of marble rocks after the application of various stress modes before fracture. *3rd WSEAS Int. Conf on Instrumentation, Measurement, Control Circuits and Systems, September 2003, Malta.*
[9] Kawashima,R., Fukase,T., Isoda,I., *Timeseries behaviour in Ac conductivity of Neodymioum Nitrate crystal with metastable phenomena*, J.Phys.Chem.Solids, 57, 5, 1996, pp. 539-545
[10] Kawashima,R., Haruki, K., Takigashira, N., Isoda, I,. *Observation on linear dynamical property of holhium nitrate crystal in low temperature region by measuring time series of ac conductivity*, Chaos, Solitons and fractals, 21, 2004, pp. 1023-1029
[11] Kleftakis, S., Agioutantis, Z., and Stiakakis, C. *Numerical simulation of the uniaxial compression test including the specimenplaten interaction*, Computational methods for shell and spatial structures, Proceedings CD-ROM, IASS-IACM, 2000.
[12] Chui, C.K., *Wavelets: a tutorial in theory and applications*, Academic Press
[13] Bentley,P., McDonnel,J., *"Wavelet transforms: an introduction",* Electr. And Comm. Eng., Aug. 1994, pp. 175-186
[14] Torrence,C., Compo, G., *A practical guide to wavelet analysis,* Bull.Amer.Meteor.Soc, 79, 1998, 61-78
[15] Theiler,J., Eubank,S., Longin,A., Galdrikan,B., Farmer,J., *Testing for nonlinearity in*

time series: the method of surrogate data, Physica D, 58, 1992, 77

[16] Popivanov,D., Mineva,A., *testing procedures for non-stationarity and non-linearity in physiological signals*, Mathematical Biosciences, 157, 1999, pp.303-320

[17] Kaplan,D., *Nonlinearity and nonstationarity, the use of surrogate data to interpreting fluctuations*, Comp. apps of Blood Pressure, Florence, Italy, May 1995, pp.1-14

[18] Bowerman,B., O'Cone,R., *time series and forecasting*, Duxbury Press, 1979, USA